Turbulence-resilient PIC-to-PIC Free Space Optical communication link

A. Martinez[1], A. Di Tria[1], F. Zanetto[1], F. Morandi[2], A. Milani[2], L. Resteghini[2] , F. Morichetti[1], and A. Melloni[1]

1. DEIB, Politecnico di Milano, via Ponzio 34/5, 20133, Milan, Italy
2. Huawei Technologies Italia Srl, Centro Direzionale Milano 2 SNC, 20054 Segrate, Italy
*andresivan.martinez@polimi.it

***Abstract*—Programmable optical processors are used to establish a chip-to-chip bidirectional Free Space Optical link operated at 25Gbit/s OOK. The link is demonstrated to be resilient to emulated turbulence over several hundred meters.**

Keyword*— *Free space optics, programmable photonics, optical processor, silicon photonics

I. INTRODUCTION

Atmospheric turbulence poses a major obstacle to achieving high-bitrate, reliable bidirectional Free Space Optical (FSO) communication [1]. Various techniques have been explored to mitigate these effects, including ultra-short pulse lasers, multi-beam transmission, structured light, orbital angular momentum beams, adaptive optics, broadband systems, hybrid configurations, and beacon-assisted multi-beam links [2].

In this paper, we present an adaptive bidirectional FSO communication system designed for resilience against atmospheric turbulence. It employs two bidirectional transceivers, each built on a silicon Photonic Integrated Circuit (PIC) featuring an Optical Antenna Array (OAA) managed by a Programmable Optical Processor (POP). The system autonomously establishes the FSO link and dynamically optimizes end-to-end power coupling. To this aim, we apply a channel labeling strategy to enable efficient bidirectional transmission using low-frequency pilot tone modulation, allowing wavelength reuse without performance degradation. Additionally, we address and resolve issues related to parasitic back reflections in the PICs. Experimental validation confirms robust 25 Gbit/s OOK signal transmission under indoor-emulated turbulence conditions.

II. PIC-TO-PIC FSO SYSTEM

Fig. 1(a) presents a simplified schematic of the PIC functioning as a transceiver. This device integrates an OAA with 16 grating couplers (GCs) and a POP composed of a binary tree of thermally tunable Mach-Zehnder interferometers (MZIs) that combine signals coherently. The PIC is realized on a silicon photonic platform and dynamically adapts in real-time to transmit and receive FSO signals while compensating for atmospheric turbulence-induced scintillation [3].

The main challenge in using two identical PICs as transceivers for a bidirectional link lies in managing parasitic back reflections from the transmitted signal. These reflections, caused by imperfections in waveguides, bends, crossings, and GCs [4], can interfere with the receiver. If reflected power exceeds the incoming signal, the PIC's control (described in [3]) may fail. To identify and quantify these reflections, we employed coherent optical frequency domain reflectometry (OFDR). Fig. 1(b) shows the normalized back reflection profile across the PIC with the highest reflection ($L = 0$ mm) corresponding to the reference fiber-to-air interface. Other peaks correspond to reflections from the MZIs, delay lines, and GCs, with GCs being the most significant contributors overall. Fig. 1(c) shows the power spectrum of the reflections. The total normalized backscattered power P_{bx} equals

$$P_{bx} = P_{bs} + 2L_{loop} - R_{ref} = 23 \text{ dB}, \quad (1)$$

where P_{bs} is the mean power of the back reflections, L_{loop} is the on-chip round-trip loss (around 6 dB), and R_{ref} is the reference fiber reflection. This indicates that, to maintain stable operation, the received optical power P_{rx} must be at most 23 dB below the transmitted power P_{tx}.

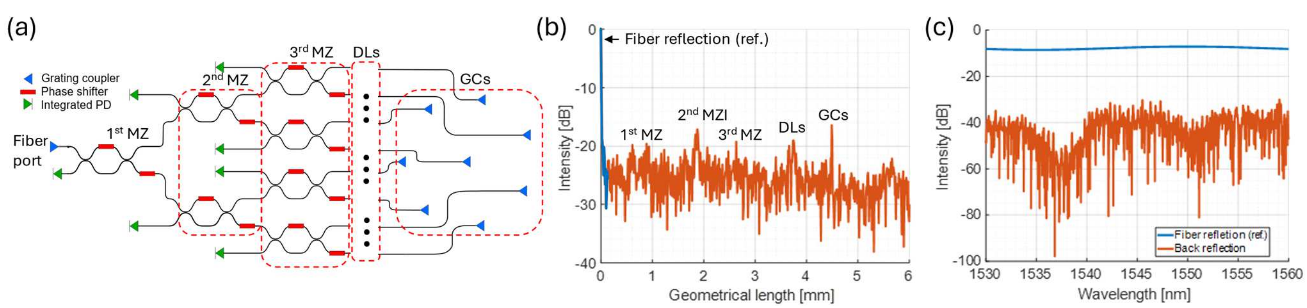

Fig. 1: (a) Simplified schematic of the PIC. (b) Backscattering vs Geometrical length of the PIC. (c) Fiber reference reflection (blue curve) and back reflection (red) spectrum of the PIC.

2025 IEEE Photonics Conference (IPC) | 979-8-3315-2559-0/25/$31.00 ©2025 IEEE | DOI: 10.1109/IPC65510.2025.11282072

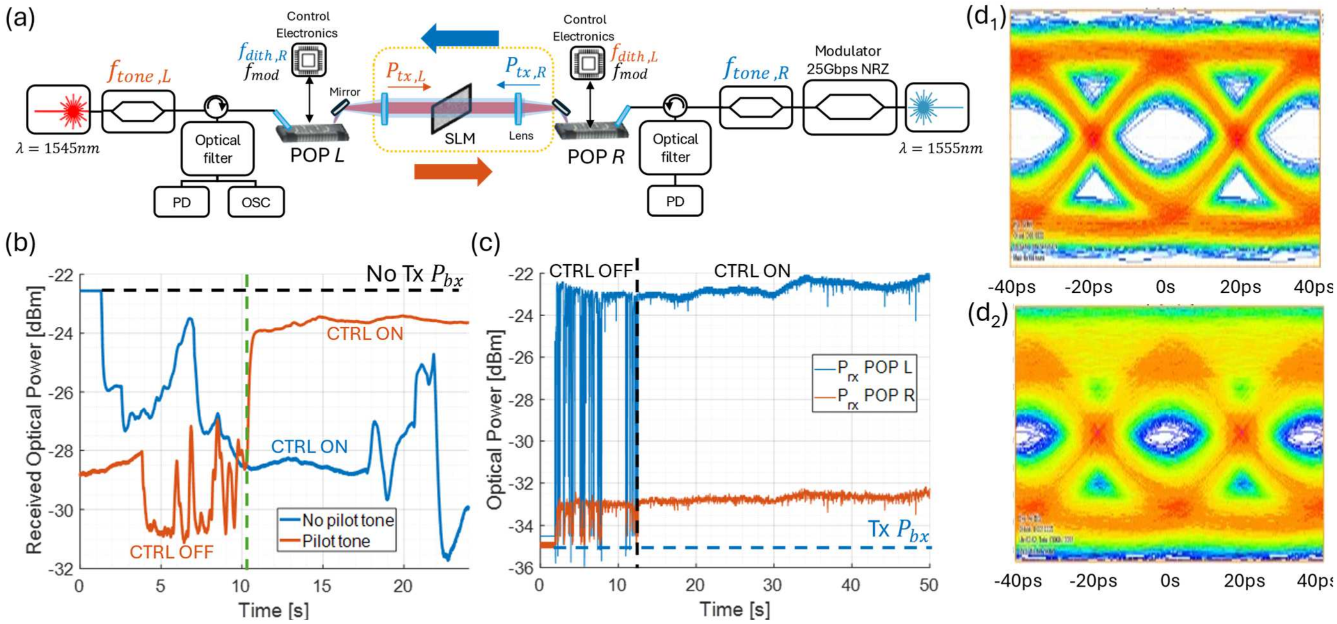

Fig. 2: (a) Schematic of the PIC-to-PIC experimental setup. (b) Received optical power P_{rx} at the left PIC (POP L) with pilot tone (orange curve), and without pilot tone (blue). (c) Received optical power P_{rx} at the POP L (blue curve) and at the POP R (orange) with the control off ($t < 12\ s$) and on ($t > 12\ s$). Eye diagram of the received 25Gb/s signal after FSO propagation: (d1) P_{rx} is higher than P_{bx}, and (d2) P_{rx} is 30 dB lower than P_{bx}.

To address this issue, a low-frequency pilot tone f_{tone} is superimposed on the transmitted signal via light intensity modulation, as shown in Fig. 2(a) [5]. This tone enables the receiver to distinguish between the transmitted and received signals, even at the same wavelength. The power margin between P_{tx} and P_{rx} increases with both the modulation depth and a lower electrical bandwidth of the measurement [5].

III. Experimental Results

The experimental setup shown in Fig. 2(a) demonstrates the adaptive PIC-to-PIC FSO link, operating at 25 Gbps using OOK modulation under simulated turbulence via a spatial light modulator (SLM) [3]. Fig. 2(b) shows that, in the absence of a pilot tone (blue curve), the received power exhibits significant fluctuations. In contrast, when the pilot tone (f_{tone} = 17,08 kHz) is applied (orange curve), the signal remains stable, with only a 1 dB penalty compared to the scenario where the PIC functions purely as a receiver (no back reflections). Fig. 2(c) displays the received optical power at the left PIC (blue curve) and the right PIC (orange curve) before and after the control system is activated (before and after $t = 12$ s, respectively). Without active control, the received power varies at both PICs, while enabling control stabilizes the signal, with only slight fading due to periodic resets of the thermal actuators. The eye diagram of the left PIC P_{rx} is shown in Fig. 2(d1) for $\mu < 8$ %.

In scenarios where the received signal is substantially weaker than back reflections, such as in long-range FSO links with high channel losses, a stronger pilot tone modulation is essential to preserve synchronization between transceivers. This scenario is typical for links spanning several hundred meters. Fig. 2(d2) presents an eye diagram for such a condition, where the received power is 30 dB lower than the reflected power. Although the increased modulation depth ($\mu > 30$ %) results in a partially closed eye diagram due to distortion, the system maintains operational performance and link stability.

Solutions to improve the power margin between P_{rx} and P_{bx} include using wavelength-selective filters in front of the integrated PDs and using microlenses on top of the GCs to reduce the geometrical loss and improve the fill factor, to increase the received power P_{rx}.

IV. Acknowledgment

The research has been carried out in the framework of the Huawei-Politecnico di Milano Joint Research Lab and the Italian National Recovery and Resilience Plan (NRRP) of NextGenerationEU, partnership on “Telecommunications of the Future” (PE0000000 - program “RESTART”, Structural Project “Rigoletto” and Focused Project “Hepic”). Part of this work was carried out at Polifab, Politecnico di Milano.

References

[1] Y. Wang, et al., “Performance analysis of an adaptive optics system for free-space optics communication through atmospheric turbulence.” *Scientific Reports* 8, 1124 (2018). https://doi.org/10.1038/s41598-018-19559-9

[2] D. McDonald, R. Bellossi, and S. Gladysz, “Field demonstration of turbulence-resilient coherent free-space optical communications over an 800 m link,” in *European Conference on Optical Communication (ECOC) 2024*, paper M3C.2.

[3] A. Martinez, et al. “Self-adaptive integrated photonic receiver for turbulence compensation in free space optical links”. *Scientific Reports* 14, 20178 (2024). https://doi.org/10.1038/s41598-024-70726-7

[4] D. Melati, A. Melloni, and F. Morichetti, "Real photonic waveguides: guiding light through imperfections," *Advances in Optics and Photonics*. 6, 156-224 (2014). https://doi.org/10.1364/AOP.6.000156

[5] D. O. M. de Aguiar et al., "Automatic Tuning of Silicon Photonics Microring Filter Array for Hitless Reconfigurable Add–Drop," in *Journal of Lightwave Technology*, vol. 37, no. 16, pp. 3939-3947, 15 Aug.15, 2019. DOI: 10.1109/JLT.2019.2916473